Efficient Simulation of Finite-Temperature Open Quantum Systems

D. Tamascelli,[1,2] A. Smirne,[1] J. Lim,[1] S. F. Huelga,[1] and M. B. Plenio[1]
[1]Institut für Theoretische Physik, Albert-Einstein-Allee 11, Universität Ulm, 89069 Ulm, Germany
[2]Dipartimento di Fisica "Aldo Pontremoli", Università degli Studi di Milano, via Celoria 16, 20133 Milano, Italy

(Received 19 December 2018; published 27 August 2019)

Chain-mapping techniques in combination with the time-dependent density matrix renormalization group are a powerful tool for the simulation of open-system quantum dynamics. For finite-temperature environments, however, this approach suffers from an unfavorable algorithmic scaling with increasing temperature. We prove that the system dynamics under thermal environments can be nonperturbatively described by temperature-dependent system-environmental couplings with the initial environment state being in its pure vacuum state, instead of a mixed thermal state. As a consequence, as long as the initial system state is pure, the global system-environment state remains pure at all times. The resulting speed-up and relaxed memory requirements of this approach enable the efficient simulation of open quantum systems interacting with highly structured environments in any temperature range, with applications extending from quantum thermodynamics to quantum effects in mesoscopic systems.

DOI: 10.1103/PhysRevLett.123.090402

Quantum systems are never completely isolated and the interaction with surrounding uncontrollable degrees of freedom can modify significantly their dynamical properties. In some cases the environment can be assumed to be memoryless, in which case master equations of Lindblad form provide an accurate effective description of the resulting open-system dynamics [1–4]. Generally, however, the description of the evolution of open quantum systems (OQSs) requires one to take into full account the environmental degrees of freedom and their interaction with the system. This becomes particularly important when the system-environment coupling is not weak and the environment reorganization process occurs on a timescale that is comparable to the system dynamics—a situation that is ubiquitous in soft or condensed matter, nanothermodynamics, and quantum biology [5–8]. In this case, the OQS dynamics is neither accessible to analytical methods (apart from very few specific instances [9–15]) nor effective master equation approaches, and more refined numerical techniques are thus needed.

Over the last two decades, a variety of numerically exact approaches for the simulation of open quantum systems have been proposed. These methods allowed for the description of features that were not accurately described by approximate methods, such as the Markov, Bloch-Redfield, or perturbative expansion techniques [2]. In particular, the time-evolving density operator with orthogonal polynomials (TEDOPA) [16,17] algorithm is a certifiable method [18] for the nonperturbative simulation of OQS that has found application for the description of a variety of open quantum systems [16,19,20]. TEDOPA belongs to the class of chain-mapping techniques [16,17,21–24] and is closely related to Lanczos tridiagonalization (see [25] and references therein); these techniques are based on a unitary mapping of the environmental modes onto a chain of harmonic oscillators with nearest-neighbor interactions. The main advantage of this mapping is the more local entanglement structure, which results in an improved efficiency of density matrix renormalization group (DMRG) methods [26]. While TEDOPA is very efficient at zero temperature, a regime that is hard to access by other methods such as hierarchical equations of motion (HEOM) [27–29] and path integral methods [30–32], its original formulation suffers from a unfavorable scaling when increasing the temperature of the bosonic bath. Because of this, other approaches, such as HEOM, are currently the method of choice in the high-temperature regime.

In this Letter, we derive a formulation of TEDOPA for finite-temperature bosonic environments that allows for its extension to arbitrary temperatures without loss of efficiency. Our approach relies on the equivalence between the reduced dynamics of an OQS interacting with a finite-temperature bosonic environment, characterized by some spectral density, and the dynamics of the same system interacting with a zero-temperature environment and a suitably modified spectral density [33–36], and further exploits fundamental properties of the theory of orthogonal polynomials [17,23,37].

Spectral density thermalization.—Consider a quantum system S interacting with a bosonic environment; for each environmental mode at frequency $\omega \geq 0$ the annihilation and creation operators a_ω, $a_\omega^\dagger$ satisfy the commutation relations $[a_\omega, a_{\omega'}^\dagger] = \delta_{\omega\omega'}, [a_\omega, a_{\omega'}] = [a_\omega^\dagger, a_{\omega'}^\dagger] = 0, \forall\, \omega, \omega' \geq 0$. The system-environment (SE) total Hamiltonian is defined by ($\hbar = 1$)

$$H_{\mathrm{SE}} = H_S + H_E + H_I \tag{1}$$

$$H_E = \int_0^{+\infty} d\omega \omega a_\omega^\dagger a_\omega; \quad H_I = A_S \otimes \int_0^{+\infty} d\omega O_\omega, \tag{2}$$

where H_S is the free system (arbitrary) Hamiltonian and H_E and H_I describe, respectively, the free evolution of the environmental degrees of freedom and the bilinear system-environment interaction [38]. In what follows we assume that O_ω is a self-adjoint operator and, in particular, is given by

$$O_\omega = \sqrt{J(\omega)} X_\omega = \sqrt{J(\omega)}(a_\omega + a_\omega^\dagger), \tag{3}$$

while A_S is a generic self-adjoint operator of the open system S. The function $J(\omega): \mathbb{R}^+ \mapsto \mathbb{R}^+$ is defined by the product of the interaction strength between the system and the environmental mode at frequency ω and the mode density and is usually referred to as the "spectral density" (SD) [2].

At time $t = 0$, system and environment are assumed to be in a factorized state $\rho_{\mathrm{SE}}(0) = \rho_S(0) \otimes \rho_E(0)$, where $\rho_S(0)$ is an arbitrary (pure or mixed) initial state of the system, $\rho_E(0) = \otimes_\omega \exp(-\beta\omega a_\omega^\dagger a_\omega)/\mathcal{Z}_\omega$ is the thermal state of the environment at inverse temperature $\beta = 1/k_B T$, and $\mathcal{Z}_\omega = \mathrm{Tr}_E[\exp(-\beta\omega a_\omega^\dagger a_\omega)]$. Under these assumptions, the open-system state $\rho_S(t) = \mathrm{Tr}_E[\rho_{\mathrm{SE}}(t)]$ at a generic time t is entirely determined by the spectral density $J(\omega)$ and the inverse temperature β [2,39–41]. In fact, $\rho_S(t)$ is fully determined by the two-time correlation function

$$\begin{aligned} S(t) &= \int_0^{+\infty} d\omega \langle O_\omega(t) O_\omega(0) \rangle_{\rho_\omega(\beta)} \\ &= \int_0^{+\infty} d\omega J(\omega) \{ e^{-i\omega t}[1 + n_\omega(\beta)] + e^{i\omega t} n_\omega(\beta) \}, \end{aligned} \tag{4}$$

where $O_\omega(t) = \exp(iH_E t) O_\omega \exp(-iH_E t)$ is the environmental interaction operator evolved at time t via the free Hamiltonian H_E and $n_\omega(\beta) = \langle a_\omega^\dagger a_\omega \rangle_{\rho_\omega(\beta)} = [\exp(\beta\omega) - 1]^{-1}$. It is then clear that, given two environments with the same two-time correlation functions, the corresponding reduced dynamics coincide [1,2,42].

If we formally extend the integral in (4) to the whole real axis and define the antisymmetrized spectral density $J^{\mathrm{ext}}(\omega) = \mathrm{sign}(\omega) J(|\omega|)$ with support on the whole real axis [43], the two-time correlation function can be reexpressed in the form

$$S(t) = \int_{-\infty}^{+\infty} d\omega \frac{J^{\mathrm{ext}}(\omega)}{2} \left[1 + \coth\left(\frac{\beta\omega}{2} \right) \right] e^{-i\omega t}. \tag{5}$$

It is crucial to note that this function can be associated with an extended bosonic environment, with positive and negative frequencies, governed by $H_{E^{\mathrm{ext}}} = \int_{-\infty}^{+\infty} d\omega \omega a_\omega^\dagger a_\omega$, which is initially in the vacuum state (i.e., $a_\omega |0\rangle \; \forall \omega \in \mathbb{R}$) and which interacts with the system via the interaction Hamiltonian $H_I(\beta) = A_S \otimes \int_{-\infty}^{+\infty} d\omega \sqrt{J_\beta(\omega)} X_\omega$, and that now involves a temperature-dependent spectral density (T-SD)

$$J_\beta(\omega) = \frac{J^{\mathrm{ext}}(\omega)}{2} \left[1 + \coth\left(\frac{\beta\omega}{2} \right) \right]. \tag{6}$$

We conclude that the reduced dynamics in the presence of an initial thermal state of the environment and a global Hamiltonian as in Eqs. (1) and (2) is the same as the one resulting from an initial vacuum state of the extended environment and a coupling governed by the new spectral density defined in Eq. (6). Note that, in contrast to previous approaches [33–36], we achieved this equivalence by suitably redefining the spectral density, which is the central object in TEDOPA. Importantly, the relationship between the original thermal chain and the pure state chain with the temperature-dependent spectral density can be formulated in terms of a unitary equivalence, which, in principle, allows one to recover the state of the full system-environment state in the original picture at any time t (see Supplemental Material [44]).

Thermalized TEDOPA.—TEDOPA [16,17,48,49] relies on the theory of orthogonal polynomials [50] to provide an analytical unitary transformation mapping the original star-shaped system-environment model into a one-dimensional configuration [17]. New modes with creation and annihilation operators $c_n^\dagger$ and c_n are defined as $c_n^{(\dagger)} = \int_0^{+\infty} d\omega U_n(\omega) a_\omega^{(\dagger)}$ using the unitary transformation $U_n(\omega) = \sqrt{J(\omega)} p_n(\omega)$, where $J(\omega)$ is an input (arbitrary) SD, and $p_n(\omega), n = 0, 1, \ldots$ are orthogonal polynomials with respect to the measure, i.e., the positive-valued function, $d\mu(\omega) = J(\omega) d\omega$ on $\mathbb{R}^+$. Thanks to the three-term recurrence relation satisfied by the orthogonal polynomials $p_n(\omega)$, the H_{SE} Hamiltonian in Eq. (1) is mapped [17] into a *chain* Hamiltonian $H^C = H_S + H_I^C + H_E^C$ with

$$\begin{aligned} H_I^C &= \kappa_0 A_S (c_0 + c_0^\dagger), \\ H_E^C &= \sum_{n=0}^{+\infty} \omega_n c_n^\dagger c_n + \sum_{n=1}^{+\infty} \kappa_n (c_n^\dagger c_{n-1} + \mathrm{H.c.}). \end{aligned} \tag{7}$$

After the unitary transformation, thus, the system interacts only with the new mode $c_0^{(\dagger)}$, and all the interactions are nearest neighbor. The mode frequencies ω_n and couplings κ_n are related to the recurrence coefficients for the polynomials $p_n(\omega)$ and can be computed either analytically or via stable numerical routines [17,37]. The crucial observation at this point is that, assuming $\int_0^{+\infty} d\omega J(\omega)/\omega < \infty$, i.e., finite reorganization energy, the temperature-dependent spectral density in Eq. (6) defines a measure

$\mu_\beta(\omega) = J_\beta(\omega)d\omega$, with support extending, by construction, over the whole real axis. Hence, there exists a family of polynomials $p_{\beta,n}$ that are orthogonal with respect to $d\mu_\beta$ and we can define the unitary transformation

$$U_{\beta,n}(\omega) = \sqrt{J_\beta(\omega)}p_{\beta,n}(\omega), \tag{8}$$

$$c^\dagger_{\beta,n} = \int_{-\infty}^{+\infty} d\omega U_{\beta,n}(\omega)a^\dagger_\omega, \tag{9}$$

and follow the same procedure as before. The resulting Hamiltonian has the same form as Eq. (7), with the modes $c_n^{(\dagger)}$ replaced by $c_{\beta,n}^{(\dagger)}$ and new coefficients $\omega_{\beta,n}$, $\kappa_{\beta,n}$ related to the polynomials $p_{\beta,n}$. The unitary transformations $U_n(\omega)$ and $U_{\beta,n}(\omega)$, respectively, determine the initial state of the chain: for standard TEDOPA, the thermal state of the environment is mapped to the thermal state of the chain $\rho_E^C(\beta) = \exp(-\beta H_E^C)/\mathcal{Z}_E^C$, while the vacuum state of the extended environment is mapped to a (factorized) vacuum pure state of the chain.

Impact on simulations.—As long as $\rho_S(0)$ is a pure state, the global state of system and chain in the T-SD approach remains pure for $\forall\, t \geq 0$. This has a major impact on the simulation of the system dynamics via time-dependent DMRG techniques [51,52], such as the time-evolving block-decimation algorithm (TEBD) [53–55]. From now on, we will refer to TEDOPA with T-SD approach as T-TEDOPA. In order to fully appreciate the advantage provided by T-TEDOPA, here we discuss the main features of its scaling properties; a more detailed comparison of the complexity of the standard and thermalized methods is reported in the Supplemental Material [44].

In order to enable computer simulations, both the length of the harmonic chain and the local dimension of the environmental oscillators must be truncated. These truncations must be chosen such that finite-size effects remain negligible during the simulation interval $[0, t_{\max}]$. For a chain of length N and local dimension d, the complexity of the standard TEDOPA approach scales as $O(Nt_{\max}(d^2\chi)^3)$, where χ is the "bond dimension," a TEBD parameter that is related to the amount of correlations in the simulated system. On the other hand, the complexity for T-TEDOPA will be given by $O(N't_{\max}(d'\chi')^3)$, where the primed letters emphasize that, in general, the local dimension, the chain length, and the bond dimension will be different from the standard case. Clearly, the reduced complexity of T-TEDOPA stems mainly from the fact that only pure states are involved in the simulation, whereas for standard TEDOPA mixed states are needed.

In addition, the local dimensions required to faithfully represent the thermal state of the chain scales unfavorably with the temperature, and as a consequence, d' can be taken significantly smaller than d (see Supplemental Material [44]). For all the dynamics taken into account here, the decrease of the local dimension in the T-TEDOPA overcompensates by itself the increase of the chain length (we usually set $N' \approx 2N$ due to an increased propagation speed in the chain) and of the bond dimension (we used at most $\chi' \approx \sqrt{2}\chi$) [44].

It is important to note that the matrix product operator (MPO) representation of the chain cannot be determined analytically, in general, and its preparation requires a considerable additional computational overhead. This step is clearly not required by T-TEDOPA, since the factorized vacuum state can be straightforwardly represented via matrix product states (MPSs). It is worth noting that the approach developed in [36] shares some features of the T-TEDOPA. It allows one to use pure instead of mixed states as well, but maps the positive and negative frequency environmental degrees of freedom into two separate chains. This results in a locally two-dimensional tensor network with a consequent considerable increase of the simulation complexity, as discussed extensively in the Supplemental Material [44]. As a last, but practically relevant observation, we note that T-TEDOPA does not require any change in the already existing and optimized TEDOPA codes, since it only needs a modification of the chain coefficients.

Case study.—In order to illustrate the main features of T-TEDOPA, we present two examples in which we consider environments with a structured SD $J_W(\omega)$, consisting of a broad background plus three Lorentzian peaks. This type of spectral density is characteristic of pigment-protein complexes, where electrically coupled pigments are subject to the structured environment provided by intrapigment and protein vibrations [56,57].

The accuracy of the results provided by T-TEDOPA is clearly apparent when comparing the simulation results with a solvable model. Consider a two-level system (TLS) subject to a pure dephasing dynamics. The environment and interaction Hamiltonians are defined as in Eqs. (2) and (3) with $A_S = (1 + \sigma_z)/2$ and $J(\omega) = J_W(\omega)$. The T-SD in Eq. (6) at $T = 0$, 77, and 300 K are shown in the inset of Fig. 1(a), while its full definition is provided in the Supplemental Material [44]. We imposed a hard cutoff $\omega_c = 350\ \mathrm{cm}^{-1}$ such that $\int_{\omega_c}^{\infty} d\omega J_W(\omega)/\omega$ becomes negligible ($< 10^{-4}\ \mathrm{cm}^{-1}$). Assume that the initial state of the TLS is a coherent superposition of the form $|+\rangle = (|0\rangle + |1\rangle)/\sqrt{2}$. In an interaction picture, the system's coherence is given by $\theta(t) = \exp[-\gamma(t)]/2$, with $\gamma(t) = \int_0^{\omega_c} d\omega J_W(\omega)\coth(\omega/2k_BT)[(1-\cos\omega t)/\omega^2]$ [2], where $\gamma(t)$ is often referred to as the decoherence function.

As clearly shown in Fig. 1(a), T-TEDOPA accurately reproduces the behavior of the coherence for $t < 1.4$ ps, with maximum error $< 10^{-4}$. As shown in Fig. 1(b), the T-TEDOPA chain coefficients depend, as expected, on the temperature T. In particular, we observe that the coupling $\kappa_{\beta,0}$ between the system and the first oscillator in the chain increases with T. For any assigned SD $J(\omega)$, we obtain

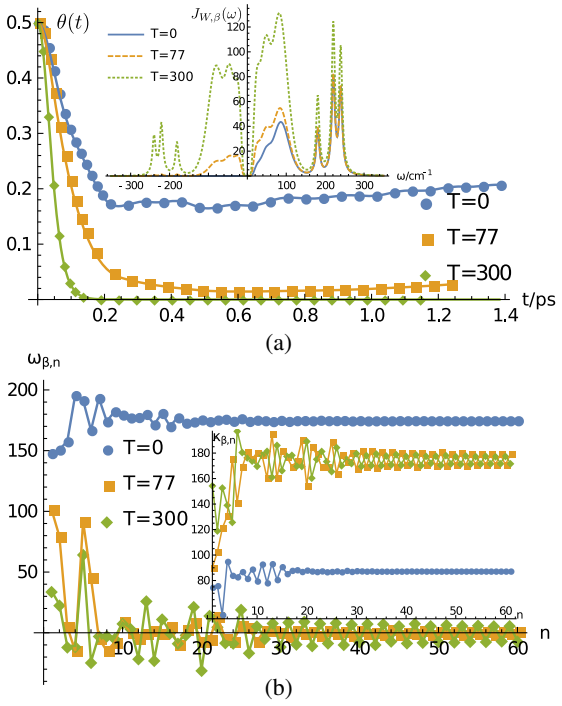

FIG. 1. (a) Coherence dynamics $\theta(t)$ for a TLS subject to pure dephasing induced by a reservoir modeled by $J_W(\omega)$ at $T = 0, 77, 300$ K. Markers represent T-TEDOPA results; analytic results, defined as in the text, are shown as solid lines. (Inset) The corresponding T-SD $J_{W,\beta}(\omega)$. (b) Chain coefficients $\omega_{\beta,n}$ and $\kappa_{\beta,n}$ (inset) corresponding to $J_{W,\beta}$ for $T = 0, 77, 300$ K.

$\kappa_{\beta,0} = ||J_\beta||_1 = \sqrt{\int_{-\omega_c}^{\omega_c} d\omega J_\beta(\omega)}$, which is a nondecreasing function of T. Moreover, the behavior of the chain parameters $\kappa_{\beta,n}$ and $\omega_{\beta,n}$ as functions of n becomes more and more jagged as T increases, inducing an effective detuning between nearest-neighboring sites in the initial part of the chain. This configuration leads to non-negligible backscattering of an excitation located initially at the first site of the chain [44]. A systematic analysis of these processes, which underpin the non-Markovian part of the dynamics, and their nontrivial temperature dependence will be the subject of a future work. Here we simply point out that this configuration results in the first sites of the T-TEDOPA chain having a higher occupation number. This allows a gradual decrease in the local dimensions d'_n of the $n = 1, \ldots, N$, which significantly reduces the simulation complexity. For example, for the simulation at $T = 300$ K, the dimension $d'_n = d'_{\max} - n(d'_{\max} - 2)/N$ with $d'_{\max} = 12$ ($\chi = 50$) led to converged results. We notice, moreover, that the chain coefficients $\omega_{\beta,n}$ and $\kappa_{\beta,n}$ tend to converge for large n to the expected asymptotic values [23,50]: if $[a(\beta), b(\beta)]$ is the support of $J_\beta(\omega)$, then $\omega_{\beta,n} \overset{n\to\infty}{\to} [a(\beta) + b(\beta)]/2$, whereas $\kappa^2_{\beta,n} \overset{n\to\infty}{\to} [b(\beta) - a(\beta)]^2/16$. Since the support is $[0, \omega_c]$ at $T = 0$ and $[-\omega_c, \omega_c]$ at $T > 0$, this means that at finite temperature T-TEDOPA will, in general, require longer chains than standard TEDOPA. This increase in length, however, leads to a constant factor increase in the T-TEDOPA complexity and is significantly overcompensated by the possibility of starting from the vacuum state. Indeed, as mentioned before, the local dimension of the standard TEDOPA scales unfavorably with the temperature, as we exemplify in Fig. 2(a) where we show the average occupation number of the chain consisting of $N = 50$ oscillators. It is clear that the minimal local dimension of the oscillator chain must be chosen much larger than the average occupation number to allow for an accurate representation of the chain thermal state. It is not surprising that the sole preparation of the chain thermal state at $T = 77$ K required one week of computation for the choice $d = 8$ (16 Intel Xeon E5-2630v3 cores), while the $T = 300$ K T-TEDOPA simulation [Fig. 1(a)] required only 8 h using the same cores (Supplemental Material [44]).

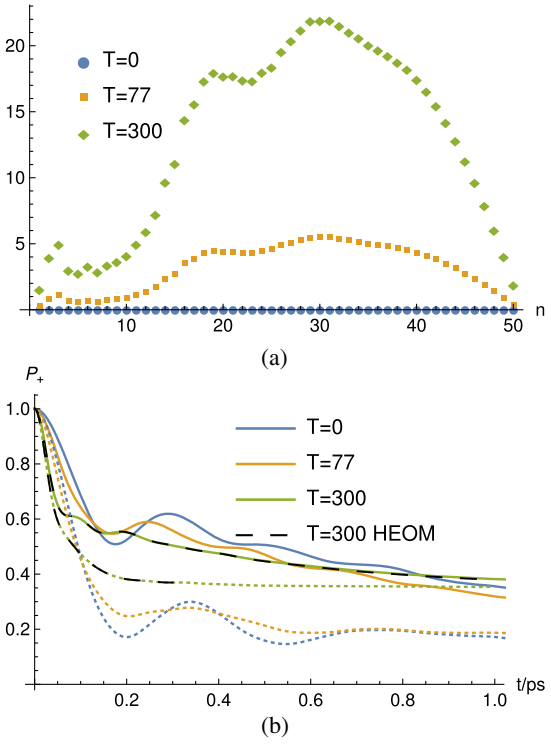

FIG. 2. (a) TEDOPA chain initialization. Average occupation number of the oscillators of a chain obtained by the standard mapping of $J_W(\omega)$; the values have been obtained via the procedure described in the Supplemental Material [44]. (b) Simulation results for a model dimeric system. The expectation value of $P_+ = |+_D\rangle\langle+_D|$ as a function of time at different temperatures shows the dynamical effect of the environmental noise on the lifetime of coherent superpositions of (electronic) quantum states. Dotted lines correspond to a structured spectral form $J_W(\omega)$, while solid lines correspond to $J'_W(\omega)$. HEOM [27–29] results are shown (dashed black lines) for comparison at 300 K (see Supplemental Material [44] for more details).

As a second example, we discuss the simulation of a form of the water-soluble chlorophyll-protein (WSCP) homodimer, a model system for the study of pigment-protein interactions and for which there exists a rather complete experimental characterization, both structurally and in terms of its linear and nonlinear optical responses [58,59]. We model the WSCP dimer as two identical TLSs with interaction Hamiltonian $H_S = H_D = \lambda\sigma_+^L\sigma_-^R + \text{H.c.}$, where $\lambda = 69\ \text{cm}^{-1}$ is the cross coupling term and $\sigma_\pm^{L,R}$ are the spin raising and lowering operators $(\sigma_x^{L,R} \pm i\sigma_y^{R,L})/2$ on the left (L) and right (R) TLS. When restricted to the single excitation subspace, H_D admits the eigenvalues $\pm 69\,\text{cm}^{-1}$ with corresponding eigenstates $|\pm_D\rangle$. Each TLS interacts with a local harmonic bath. The two baths are independent but described by the same spectral density $J_W(\omega)$ used so far. The interaction Hamiltonian is $H_I = H_I^L + H_I^R$ with $H_I^{L(R)}$ defined as in Eq. (2) with $A_S^{L(R)} = (1 + \sigma_z^{L(R)})/2$. Since the overall Hamiltonian conserves the excitation number, the evolved state belongs to the space spanned by $|\pm_D\rangle$. Figure 2(b) shows the evolution of the projection $P_+ = |+_D\rangle\langle+_D|$ as a function of time, when the system starts from $\rho_S(0) = |+_D\rangle\langle+_D|$, for two different spectral densities, namely, the full spectral density $J_W(\omega)$ and $J'_W(\omega)$ where only the background is considered. The simulation at 300K required $d'_{\text{max}} = 20$, $\chi = 180$. A detailed discussion of the influence of the Lorentzian contribution to the reduced system dynamics and the comparison with actual experiments is beyond the scope of this Letter, but our results already show the capability of the method to make predictions across the whole temperature range and for highly structured spectral densities.

Conclusion and outlook.—In this Letter, we have presented a new method, T-TEDOPA, for the efficient, accurate, and certifiable simulation of open quantum system dynamics at arbitrary temperatures. The central insight was a suitable redefinition of the environmental spectral density, which allowed for the use of a zero-temperature environment in place of a finite-temperature environment without affecting the system dynamics. This allows for using MPSs in place of MPO for the description of the harmonic chain of environmental oscillators. As a consequence, we obtain a significant reduction in the scaling of the algorithmic complexity as compared to state-of-the-art chain-mapping techniques and orders of magnitude reductions in computation time. By construction, T-TEDOPA can be implemented as a plug-in procedure by the already existing and highly optimized TEDOPA codes, which can now be used to efficiently simulate open quantum system dynamics across the entire temperature range.

Our approach is particularly relevant whenever one wants to provide a quantitative description of open-system dynamics in the presence of structured and nonperturbative environments, such as those commonly encountered in quantum biology [5], nanoscale thermodynamics [60], or condensed-matter systems [38], as well as in situations where the effect of environmental noise has to be identified accurately to discriminate it from possible fundamental decoherence in high-precision tests of the quantum superposition principle [61,62] or be exploited as a building block in other methods, such as the transfer tensor scheme [63,64]. Future research will be devoted to the extension of the T-TEDOPA method to more general types of system-bath interactions.

We thank Felipe Caycedo-Soler and Ferdinand Tschirsich for many useful discussions; we acknowledge support by the ERC Synergy Grant BioQ, the QuantERA project NanoSpin, the EU projects AsteriQS and HYPERDIAMOND, the BMBF projects DiaPol, the John Templeton Foundation, and the CINECA-LISA project TEDDI.

[1] H. Carmichael, *An Open Systems Approach to Quantum Optics* (Springer-Verlag, Berlin, 1993).
[2] H.-P. Breuer and F. Petruccione, *The Theory of Open Quantum Systems* (Oxford University Press, Oxford, 2002).
[3] C. W. Gardiner and P. Zoller, *Quantum Noise: A Handbook of Markovian and Non-Markovian Quantum Stochastic Methods with Applications* (Springer, Berlin, 2004).
[4] A. Rivas and S. F. Huelga, *Open Quantum Systems* (Springer, New York, 2012).
[5] S. F. Huelga and M. B. Plenio, Contemp. Phys. **54**, 181 (2013).
[6] A. Rivas, S. F. Huelga, and M. B. Plenio, Rep. Prog. Phys. **77**, 094001 (2014).
[7] H.-P. Breuer, E.-M. Laine, J. Piilo, and B. Vacchini, Rev. Mod. Phys. **88**, 021002 (2016).
[8] I. de Vega and D. Alonso, Rev. Mod. Phys. **89**, 015001 (2017).
[9] J. Luczka, Physica (Amsterdam) **167A**, 919 (1990).
[10] B. L. Hu, J. P. Paz, and Y. Zhang, Phys. Rev. D **45**, 2843 (1992).
[11] B. M. Garraway, Phys. Rev. A **55**, 2290 (1997).
[12] J. Fischer and H.-P. Breuer, Phys. Rev. A **76**, 052119 (2007).
[13] A. Smirne and B. Vacchini, Phys. Rev. A **82**, 022110 (2010).
[14] L. Diósi and L. Ferialdi, Phys. Rev. Lett. **113**, 200403 (2014).
[15] L. Ferialdi, Phys. Rev. Lett. **116**, 120402 (2016).
[16] J. Prior, A. W. Chin, S. F. Huelga, and M. B. Plenio, Phys. Rev. Lett. **105**, 050404 (2010).
[17] A. W. Chin, A. Rivas, S. F. Huelga, and M. B. Plenio, J. Math. Phys. (N.Y.) **51**, 092109 (2010).
[18] M. P. Woods, M. Cramer, and M. B. Plenio, Phys. Rev. Lett. **115**, 130401 (2015).
[19] J. Prior, I. de Vega, A. W. Chin, S. F. Huelga, and M. B. Plenio, Phys. Rev. A **87**, 013428 (2013).
[20] A. W. Chin, J. Prior, R. Rosenbach, F. Caycedo-Soler, S. F. Huelga, and M. B. Plenio, Nat. Phys. **9**, 113 (2013).
[21] K. Hughes, C. Christ, and I. Burghardt, J. Chem. Phys. **131**, 024109 (2009).

[22] R. Martinazzo, B. Vacchini, K. Hughes, and I. Burghardt, J. Chem. Phys. **134**, 011101 (2011).
[23] M. P. Woods, R. Groux, A. W. Chin, S. F. Huelga, and M. B. Plenio, J. Math. Phys. (N.Y.) **55**, 032101 (2014).
[24] L. Ferialdi and D. Dürr, Phys. Rev. A **91**, 042130 (2015).
[25] I. de Vega, U. Schollwöck, and F. A. Wolf, Phys. Rev. B **92**, 155126 (2015).
[26] S. R. White, Phys. Rev. Lett. **69**, 2863 (1992).
[27] Y. Tanimura and R. Kubo, J. Phys. Soc. Jpn. **58**, 101 (1989).
[28] A. Ishizaki and G. R. Fleming, J. Chem. Phys. **130**, 234111 (2009).
[29] Y. Tanimura, J. Phys. Soc. Jpn. **75**, 082001 (2006).
[30] R. P. Feynman, Rev. Mod. Phys. **20**, 367 (1948).
[31] N. Makri, Chem. Phys. Lett. **193**, 435 (1992).
[32] P. Nalbach, J. Eckel, and M. Thorwart, New J. Phys. **12**, 065043 (2010).
[33] L. Diósi, N. Gisin, and W. T. Strunz, Phys. Rev. A **58**, 1699 (1998).
[34] T. Yu, Phys. Rev. A **69**, 062107 (2004).
[35] M. Blasone, P. Jizba, and G. Vitiello, *Quantum Field Theory and Its Macroscopic Manifestations: Boson Condensations, Ordered Patterns and Topological Defects* (World Scientific, Singapore, 2011).
[36] I. de Vega and M.-C. Bañuls, Phys. Rev. A **92**, 052116 (2015).
[37] W. Gautschi, ACM Trans. Math. Softw. **20**, 21 (1994).
[38] A. J. Leggett, S. Chakravarty, A. T. Dorsey, M. P. A. Fisher, A. Garg, and W. Zwerger, Rev. Mod. Phys. **59**, 1 (1987).
[39] R. P. Feynman and F. L. Vernon, Ann. Phys. (N.Y.) **24**, 118 (1963).
[40] N. G. van Kampen, Physica (Amsterdam) **74**, 215 (1974).
[41] G. Gasbarri and L. Ferialdi, Phys. Rev. A **97**, 022114 (2018).
[42] D. Tamascelli, A. Smirne, S. F. Huelga, and M. B. Plenio, Phys. Rev. Lett. **120**, 030402 (2018).
[43] V. May and P. Kühn, *Charge and Energy Transfer Dynamics in Molecular Systems* (Wiley-VCH, Weinheim, 2004).
[44] See Supplemental Material at http://link.aps.org/supplemental/10.1103/PhysRevLett.123.090402 for more details about the estimation of the length and local dimension of the chain, the excitation dynamics of the first sites, the WSCP spectral density and the comparison of T-TEDOPA with standard TEDOPA and the thermofield approach, which includes Refs. [45–47].
[45] U. Schollwöck, Ann. Phys. (Amsterdam) **326**, 96 (2011).
[46] A. M. Rosnik and C. Curutchet, J. Chem. Theory Comput. **11**, 5826 (2015).
[47] J. Lim, C. M. Bösen, A. D. Somoza, C. P. Koch, M. B. Plenio, and S. F. Huelga, arXiv:1812.11537.
[48] D. Tamascelli, R. Rosenbach, and M. B. Plenio, Phys. Rev. E **91**, 063306 (2015).
[49] L. Kohn, F. Tschirsich, M. Keck, M. B. Plenio, D. Tamascelli, and S. Montangero, Phys. Rev. E **97**, 013301 (2018).
[50] W. Gautschi, *Orthogonal Polynomials Computation and Approximation* (Oxford Science Publications, Oxford, 2004).
[51] S. R. White and A. E. Feiguin, Phys. Rev. Lett. **93**, 076401 (2004).
[52] S. Rommer and S. Östlund, Phys. Rev. B **55**, 2164 (1997).
[53] G. Vidal, Phys. Rev. Lett. **91**, 147902 (2003).
[54] G. Vidal, Phys. Rev. Lett. **93**, 040502 (2004).
[55] M. Zwolak and G. Vidal, Phys. Rev. Lett. **93**, 207205 (2004).
[56] S. Chandrasekaran, Aghtar, A. Valleau, M. S. Aspuru-Guzik, and U. Kleinekathöfer, J. Phys. Chem. B **119**, 9995 (2015).
[57] C. Olbrich, J. Strümpfer, K. Schulten, and U. Kleinekathöfer, J. Phys. Chem. Lett. **2**, 1771 (2011).
[58] G. Renger, J. Pieper, C. Theiss, I. Trostmann, H. Paulsen, T. Renger, H. Eichler, and F.-J. Schmitt, Journal of plant physiology **168**, 1462 (2011).
[59] J. Alster, H. Lokstein, J. Dostál, A. Uchida, and D. Zigmantas, J. Phys. Chem. B **118**, 3524 (2014).
[60] S. Vinjanampathy and J. Anders, Contemp. Phys. **57**, 545 (2016).
[61] A. Bassi, K. Lochan, S. Satin, T. P. Singh, and H. Ulbricht, Rev. Mod. Phys. **85**, 471 (2013).
[62] M. Arndt and K. Hornberger, Nat. Phys. **10**, 271 (2014).
[63] J. Cerrillo and J. Cao, Phys. Rev. Lett. **112**, 110401 (2014).
[64] R. Rosenbach, J. Cerrillo, S. F. Huelga, J. Cao, and M. B. Plenio, New J. Phys. **18**, 023035 (2016).